Effects of the Trapezoidal Embedded Loading Berm on the Stability of Soft-Soil Foundation Embankment

Feng Xiong[1,2,*], Yuexiang Wang[1], Fan Yang[1], Lang Zhou[3], Caifeng Hu[1], Xuebing Wang[1] and Fan Li[1]

[1] College of Civil Engineering, Hefei University of Technology, Hefei, 230009, China

[2] Xinjiang Key Laboratory of Geohazard Prevention, Xinjiang Institute of Engineering, Urumchi, 830023, China

[3] Agroecosystem Sustainability Center, Institute for Sustainability, Energy, and Environment, University of Illinois Urbana-Champaign, Urbana, IL 61801, USA

INFORMATION

Keywords:
Soft-soil foundation embankment
trapezoidal embedded loading berm
stability coeffcient
orthogonal test

DOI: 10.23967/j.rimni.2025.10.65838

SCIPEDIA Revista Internacional de Métodos Numéricos para Cálculo y Diseño en Ingeniería

RIMNI

Effects of the Trapezoidal Embedded Loading Berm on the Stability of Soft-Soil Foundation Embankment

Feng Xiong[1,2,*], **Yuexiang Wang**[1], **Fan Yang**[1], **Lang Zhou**[3], **Caifeng Hu**[1], **Xuebing Wang**[1] **and Fan Li**[1]

[1]College of Civil Engineering, Hefei University of Technology, Hefei, 230009, China

[2]Xinjiang Key Laboratory of Geohazard Prevention, Xinjiang Institute of Engineering, Urumchi, 830023, China

[3]Agroecosystem Sustainability Center, Institute for Sustainability, Energy, and Environment, University of Illinois Urbana-Champaign, Urbana, IL 61801, USA

ABSTRACT

The traditional loading berm is effective in reinforcing soft-soil foundation embankments, however, it is found that its large footprint limits its application in some narrow construction sites in recent years. Therefore, to address this limitation, the trapezoidal embedded loading berm (TELB) has been introduced, and its feasibility was examined in this paper. Firstly, an analytical model was developed to investigate the mechanical behavior of the TELB. Then, a numerical approach was employed to assess the TELB's efficacy in enhancing the stability of soft-soil foundation embankments. The study elucidates the impact of various TELB parameters—such as slope angle, lower edge width, height, density, internal friction angle, and cohesion—on the embankment stability coefficient. Finally, an orthogonal test was conducted to evaluate the sensitivity of each parameter concerning embankment stability. The results demonstrate that the TELB substantially improves the stability of soft-soil foundation embankments, with stability coefficients increasing as the geometric and physical-mechanical parameters of the loading berm are enhanced. Among the parameters, height and density exert a more pronounced effect on the stability coefficient compared to cohesion and internal friction angle. This research provides valuable insights for the design and construction of TELBs and contributes to mitigating the environmental impact of road construction in soft soil regions.

OPEN ACCESS

Received: 23/03/2025

Accepted: 10/06/2025

Published: 27/10/2025

DOI
10.23967/j.rimni.2025.10.65838

Keywords:
Soft-soil foundation embankment
trapezoidal embedded loading berm
stability coefficient
orthogonal test

1 Introduction

Soft soil deposits are extensively distributed throughout China's coastal regions. It has characteristics of high water content, low strength, and strong compressibility [1–3]. During the construction of expressways in soft soil areas, the embankment may be prone to uneven settlement and even instability [4–6].

*Correspondence: Feng Xiong (cvexf@hfut.edu.cn).

The loading berm is a technique employed for reinforcing soft-soil foundation. Numerous studies have investigated the effectiveness of loading berms in enhancing the stability of soft-soil foundation embankments. Huang et al. [7] demonstrated that under significant shear stress, vertical soil settlement is influenced by the combined effects of drainage consolidation and lateral deformation. Loading berms can enhance shear stress levels and effectively reduce both vertical and lateral settlement. Li et al. [8] found that using loading berms not only mitigates lateral displacement but also increases the critical height of the embankment and accelerates construction processes. Corkum and Martin [9] identified that a small berm at the foot of a slope can effectively control landslide displacement. According to the physical modeling and monitoring results, Zaytesv et al. [10] found that the embankment settlement can be effectively decreased by increasing the height of the loading berm. Liu and Wang [11] found that the strength reduction method is more appropriate than the ultimate load method for analyzing the stability of the embankment with loading berms. Zhu [12] examined the optimal height for loading berms and compared their stability and spatial requirements with those of slope cutting. Zhao et al. [13] developed an equilibrium equation that accounts for the combined effects of cohesion and internal friction angle on the sliding surface, discussing the optimal width and height of loading berms. Chen and Song [14] put forward an optimization design method for single-stage loading berms to reinforce the high-filling slopes and introduced a simplified method for calculating three typical landslide surface stability coefficients. Viswanadham et al. [15] studied the seepage stability of the railway embankment with fly ash as filling materials, recommending a minimum loading berm height of 1.5 m for embankments up to 11 m in height.

The construction of expressways on soft-soil foundations often necessitates the use of loading berms to enhance stability. However, the traditional loading berms require substantial land area, which can be problematic in regions with limited land resources, such as agricultural zones. To address this challenge, Zhang et al. [16] proposed and verified the use of the embedded loading berm as a means to reinforce soft-soil foundation. Xiong et al. [17] examined the relationship between the width and height of embedded loading berms and the embankment stability coefficient, finding that stability is positively correlated with both the width and the square of the height of the embedded loading berm. Additionally, they analyzed the sensitivity of various parameters of rectangular embedded loading berms on embankment stability.

While some research has been conducted on rectangular embedded loading berms, which are theoretically feasible but challenging to construct—particularly when high excavation depths are required, potentially leading to pit wall collapse—this paper introduces the trapezoidal embedded loading berm (TELB) as an alternative. The study verifies the feasibility of the TELB and investigates how its parameters influence embankment stability. Finally, the sensitivity of TELB parameters on embankment stability is evaluated using an orthogonal test. This research contributes to the design and construction of TELBs and aims to reduce the environmental impact of road construction projects.

2 Analytical Model for the Soft-Soil Foundation Embankment Reinforced by TELB

The analytical model flowchart is demonstrated in Fig. 1. The TELB is used to reduce lateral displacement in soft-soil embankments, thereby enhancing their stability. However, if the strength of the TELB falls short of the required specifications, it may result in shear failure, as illustrated in Fig. 2. The failure modes analyzed in this study were determined based on mechanical criteria.

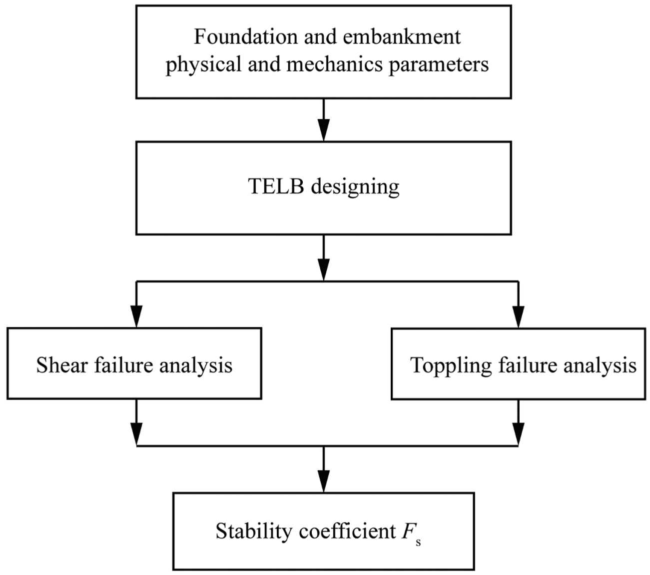

Figure 1: The flowchart of analytical model

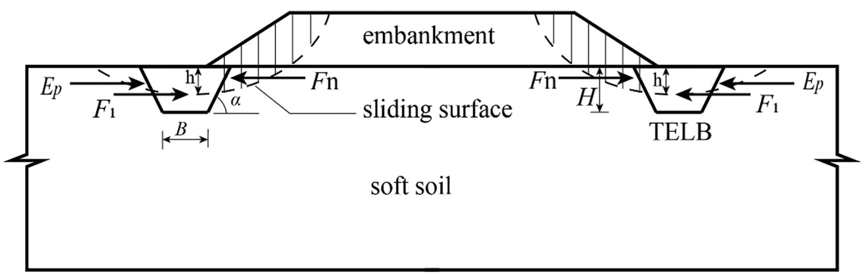

Figure 2: Shear failure diagram of the TELB

The force F_1 is the cohesion and friction on the sliding surface; E_p is the passive earth pressure in front of the TELB; and F_n is the landslide thrust force. These parameters can be presented as follows.

$$F_1 = \left(B + 2\frac{H-h}{\tan\alpha}\right)c + \left(B + 2\frac{H-h}{\tan\alpha}\right)h\rho\tan\varphi \tag{1}$$

$$F_n = F_{n-1}\psi_n + F_s G_n \sin\beta_n - G_n\cos\beta_n\tan\varphi_n - c_n l_n \tag{2}$$

$$E_p = \frac{\gamma h^2 K_p}{2} + 2ch\sqrt{K_p} \tag{3}$$

where γ is unit weight; ρ is the density of the TELB; h is the height of the TELB above the sliding surface; c is the cohesion of the TELB; φ is the internal friction angle of the TELB; B is the lower edge width of the TELB; H is the height of the TELB; α is the TELB slope angle; F_n, F_{n-1} is the residual sliding force of block n and block $n-1$; Ψ_n is the transfer coefficient; G_n is the weight of the block n; β_n is the slope angle of the block n at the sliding surface; l_n is the length of the block n along the sliding surface; K_p is the passive earth pressure coefficient; F_s is the stability factor.

When the TELB is in a critical state, the following equation is obtained:

$$F_n = F_1 + E_p \tag{4}$$

Substituting Eqs. (1)–(3) into Eq. (4), the Eq. (5) was obtained.

$$Fs = \frac{\left(B(c + h\rho \tan\varphi) + 2\frac{H-h}{\tan\alpha}(c + h\rho\tan\varphi) + P\right)}{G_n \sin\beta_n} \tag{5}$$

where:

$$P = G_n \ \cos \ \beta_n tan\ \varphi + l_n c_n + \frac{\gamma h^2 K_p^2}{2} + 2chK_p - F_{n-1}\psi_n$$

According to Eq. (5), it can be seen that the embankment stability coefficient F_s exhibits a positive correlation with the TELB lower edge width, height, density, cohesion, and internal friction angle. As these parameters increase, the embankment stability coefficient F_s also increases. Conversely, the embankment stability coefficient F_s shows a negative correlation with the slope angle of the sliding surface; thus, the stability coefficient decreases as the TELB slope angle increases.

As illustrated in Fig. 3, if the TELB possesses sufficient shear strength, it can effectively prevent shear failure. However, excessive landslide thrust forces may lead to the toppling failure of the TELB.

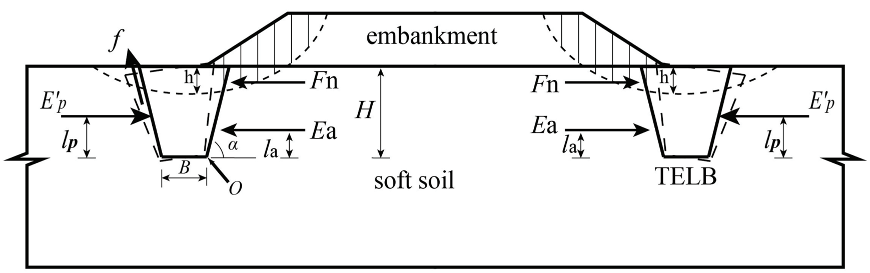

Figure 3: Diagram of the TELB overturn failure

The active earth pressure on the TELB is presented as E_a; the passive earth pressure is presented as E'_p; The friction between TELB and the soft soil is presented as f. Then, the following equations are obtained.

$$E'_p = \frac{\gamma H^2 K_p}{2} + 2cH\sqrt{K_p} \tag{6}$$

$$E_a = \frac{\gamma H^2 K_a}{2} - 2cH\sqrt{K_a} + \frac{2c^2}{\gamma} \tag{7}$$

$$l_p = \frac{H}{3}\frac{\gamma HK_p + 6c\sqrt{K_p}}{\gamma HK_p + 4c\sqrt{K_p}} \tag{8}$$

$$l_a = \frac{\gamma HK_a - 2c\sqrt{K_a}}{3\gamma K_a} \tag{9}$$

$$f = c_1 \frac{H}{\sin\alpha} B + E_p \tan\varphi_1 \tag{10}$$

where the l_p is the distance between the point of action of the passive earth pressure and the lower edge of the TELB, l_a is the distance between the point of active earth pressure action and the lower edge of the TELB, f is the friction between TELB and soft soil, c_1 and φ_1 are the cohesion and the angle of internal friction between the TELB and the soft soil.

When the TELB is in a critical state, the torque at point O on the TELB equals zero. Then,

$$E_p' l_p + fB\cos\alpha + F_n\left(H - \frac{h}{2}\right) + E_a l_a \tag{11}$$

Given h is considerably smaller than H, $H - h/2$ can be approximated as H. By substituting Eqs. (6)–(10) into Eqs. (11), (12) is derived.

$$F = \frac{PH^2 + QH + R + \dfrac{S}{H}}{G_n \sin\beta_n} + \frac{\gamma K_p \cos\alpha}{2G_n \sin\beta_n} HB + \frac{\dfrac{c_1}{\tan\alpha} + 2c\sqrt{K_p}\cos\alpha}{G_n H \sin\beta_n} B \tag{12}$$

where:

$$P = \frac{\gamma}{6}\left(\frac{\gamma HK_p + 6c\sqrt{K_p}}{\gamma HK_p + 4c\sqrt{K_p}} \cdot K_p - K_a\right)$$

$$Q = \frac{2c\sqrt{K_p}}{3}\left(\frac{\gamma HK_p + 6c\sqrt{K_p}}{\gamma HK_p + 4c\sqrt{K_p}} + c\sqrt{K_a}\right)$$

$$R = \frac{2c^2}{\gamma} + c_n l_n + G_n \cos\beta_n \tan\varphi_n$$

$$S = \frac{4c^3}{3\gamma^2\sqrt{K_a}}$$

The polynomial coefficients P and Q are functions of H, but they exhibit minimal variation within a specific range, allowing them to be treated as constants. Eq. (12) indicates that the embankment stability coefficient (F_s) is positively correlated with the height H, lower edge width B, and cohesion c of TELB, but it negatively correlates with the TELB slope angle α.

The above derivation process outlined involves several assumptions. For example, the soil pressure on the TELB is regarded as a horizontal force, and the support is provided by the soft soil beneath it. Consequently, further numerical simulation studies are required to address these assumptions and refine the analysis.

3 Numerical Simulation of the Soft-Soil Foundation Embankment Stability Reinforced by TELB

3.1 Numerical Models

To evaluate the feasibility of the trapezoidal embedded loading berm (TELB) for reinforcing the soft-soil foundation embankment, a numerical model was developed using FLAC3D software 5.0. As shown in Fig. 4, the model dimensions are 91 m in length, 20 m in width, and 26 m in height. The soft-soil foundation has a height of 20 m, while the embankment has a height of 6 m. The lengths of the top and bottom surfaces of the embankment are 33 and 51 m, respectively. The model dimensions were determined according to practical engineering. The TELB is embedded into the foundation.

In the model, the bottom boundary is constrained in all directions, the left and right boundaries are fixed in the X-direction, and the front and rear boundaries are fixed in the Y-direction. The physical and mechanical parameters used in the model are detailed in Table 1.

To investigate the influences of the TELB geometric and mechanical parameters on the embankment stability, the stability coefficients of the embankment are calculated by the strength reduction method. The numerical calculations were performed employing FLAC software 5.0.

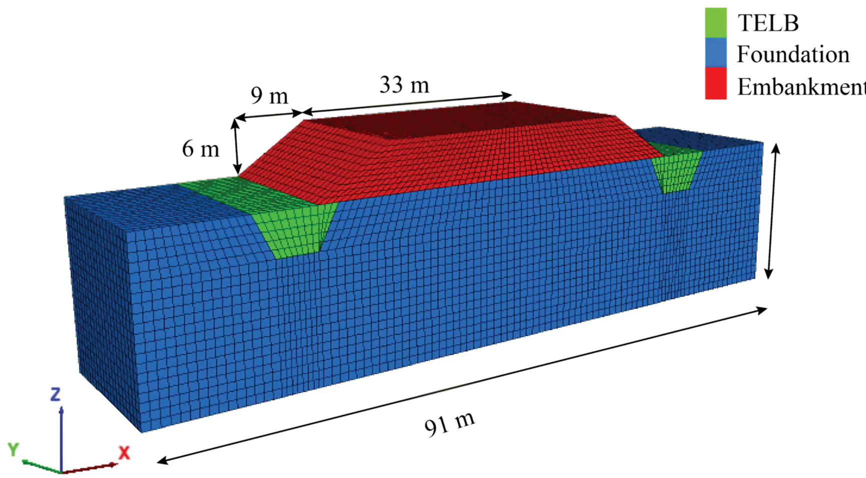

Figure 4: Numerical calculation model of TELB

By the Mohr-Coulomb (MC) failure criterion, the shear strength (τ_f) is given by:

$$\tau_f = \sigma \ tan \ \phi + c \tag{13}$$

where φ is the friction angle and c is the effective cohesion, which is shear strength parameters; σ is the normal stress.

Table 1: Physical and mechanical parameters of the model

Type	Density $\rho/(\text{kg}\cdot\text{m}^{-3})$	Elastic modulus E/MPa	Cohesion c/Pa	Internal friction angle φ/°	Poison ratio v
Soft foundation soil	1700	5	8000	6	0.35
Embankment	1900	20	20,000	24	0.30

The strength reduction method involves progressively reducing the soil's shear strength parameters until failure occurs in the embedded loading berms. The corresponding strength reduction factor (SRF) at this critical state represents the stability factor of the embedded loading berms. The reduced shear strength is then given by:

$$c' = \frac{c}{SRF} \tag{14}$$

$$\phi' = tan^{-1}\frac{tan \ \phi}{SRF} \tag{15}$$

$$\tau_f' = \sigma \ tan \ \phi' + c' \tag{16}$$

The analysis begins with an initial SRF set to a reasonably low value. Through iterative adjustments, the SRF is progressively increased until failure occurs in the embedded loading berm, at which point the final SRF is taken as the stability factor.

The parameters for this analysis include a TELB slope angle ranging from 45° to 85°, a lower edge width varying between 3 and 12 m, a height ranging from 2 to 6 m, a density between 1700 and 2100 kg/m^3, a cohesion varying from 10 to 20 kPa, and an internal friction angle spanning from 8° to 24° [18].

3.2 Stability Coefficient of Embankment with Trapezoidal and Rectangular Embedded Loading Berms

Table 2 shows the dimensions of the embedded loading berm for every case. Using the strength reduction method, the stability coefficients of the embankment are obtained and are listed in Table 3. For the embankment without the embedded loading berm (Case 0), the stability coefficient is 1.03. When the embankment is reinforced with a rectangular embedded loading berm (Case 1), the stability coefficient increases to 1.20, representing a 16.50% improvement over Case 0.

Table 2: Embedded loading berm dimensions for every case

	Case 0	Case 1	Case 2	Case 3	Case 4
Upper edge width	–	8 m	10 m	12 m	15 m
Lower edge width	–	8 m	6 m	8 m	12 m
Height	–	5 m	5 m	4 m	3 m

Note: There is no embedded loading berm for case 0. The embedded loading berm volume is the same or similar for Case 1∼Case 4. The embedded loading berm materials are the same as those of the embankment. The values of the parameters are from references [17,18].

Table 3: The stability coefficients of the embankment for different cases

Type	Case 0	Case 1	Case 2	Case 3	Case 4
F_s	1.03	1.20	1.20	1.20	1.21
Growth rate/%	–	16.50	16.50	16.50	17.48

Note: There is no embedded loading berm for case 0. The embedded loading berm volume is the same or similar for Case 1∼Case 4. F_s is the stability coefficients.

In Cases 2 and 3, the stability coefficients are both 1.20, which is also 16.50% higher than that of Case 0. In Case 4, the stability coefficient is 1.20, reflecting a 17.48% increase compared to Case 0. These results demonstrate that the embedded loading berm significantly enhances the stability of the soft-soil foundation embankment.

The stability coefficients for Cases 1 through 4 are either similar or identical. This suggests that when the cross-sectional areas of the trapezoidal embedded loading berm (TELB) and the rectangular embedded loading berm (RELB) are equivalent, their reinforcement effects are comparable. Given the challenges associated with construction and the stability of pits in soft-soil foundations, the TELB is relatively more suitable for reinforcing soft-soil foundation embankments.

3.3 Effects of Trapezoidal Embedded Loading Berm (TELB) on the Stability Coefficient

Figs. 5 and 6 present the influences of the TELB's geometric and mechanical parameters on the embankment stability coefficients.

As depicted in Fig. 5a, the stability coefficients of the embankment decrease as the slope angle increases. Fig. 5b shows that the stability coefficients rise linearly with increasing TELB height, with noticeable increments. This is in agreement with the analytical results in Section 2. Fig. 5c illustrates that the stability coefficients generally increase linearly with an increase in the TELB lower edge width. When the lower edge width of the TELB exceeds 6 m, the stability coefficients plateau. This suggests that the height of the TELB has a more pronounced effect on embankment stability.

Figs. 6a and 5c indicate that the effects of TELB density and lower edge width on embankment stability coefficients are comparable. According to Fig. 6b,c, variations in cohesion and internal friction angle result in minimal changes to the embankment's stability coefficients, suggesting that these parameters have a negligible impact on stability.

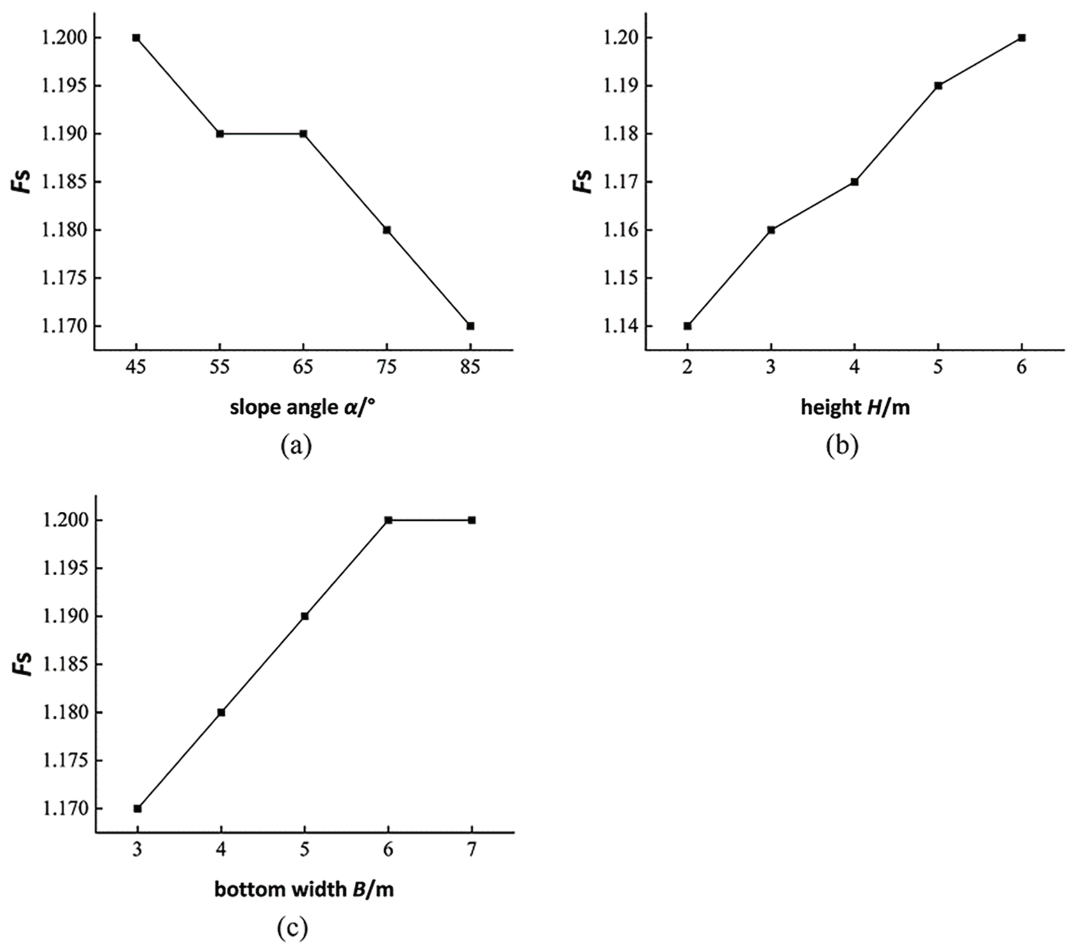

Figure 5: Influence of the TELB geometric parameters on the stability coefficient. (a) Slope angle α. (b) Height H. (c) Lower edge width B

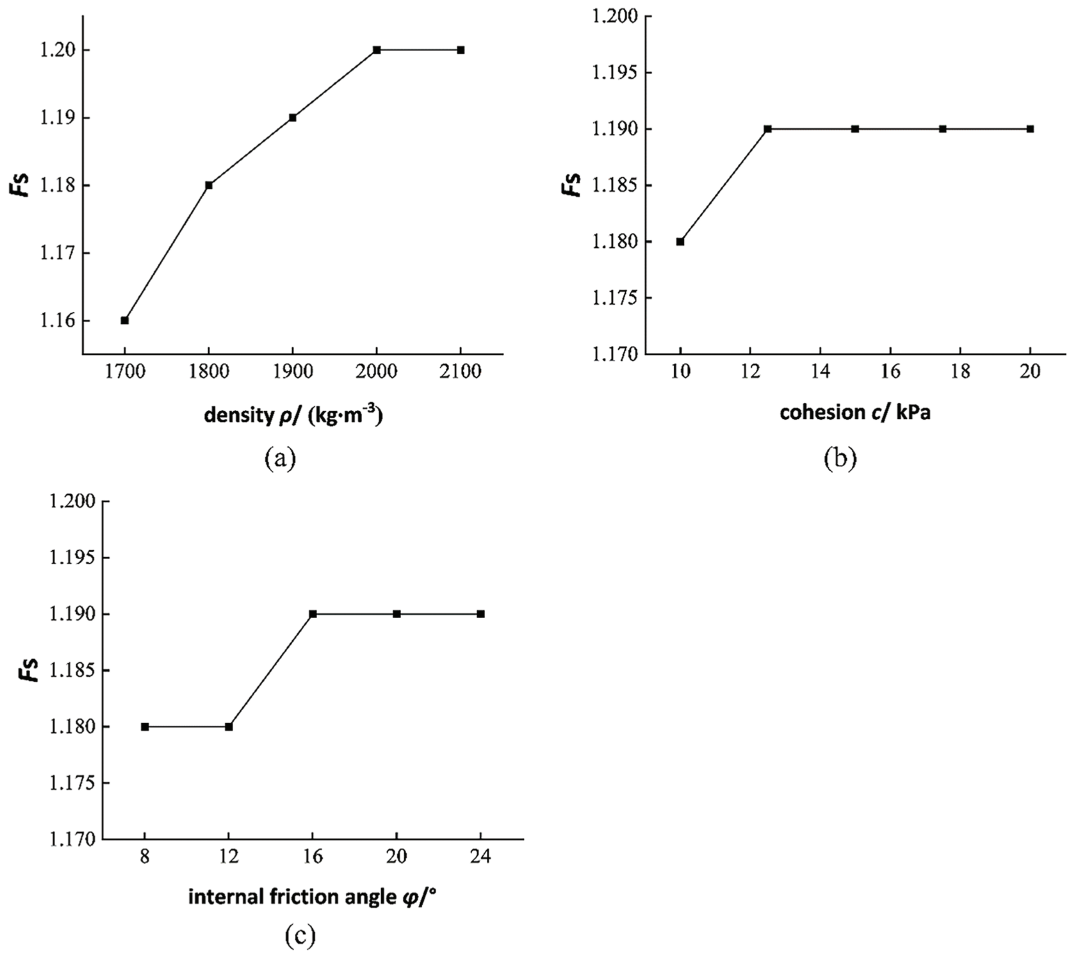

Figure 6: Influence of the TELB geometric parameters on the stability coefficient. (a) Density ρ. (b) Cohesion c. (c) Internal friction angle φ

When the TELB slope angle (α) is 65°, the lower edge width (B) is 6 m, and the height (H) is 5 m, the embankment stability coefficient (F_s) is 1.20, which meets the stability requirements. Therefore, the TELB can be designed with a slope angle of 65°, a lower edge width of 6 m, and a height of 5 m.

4 Parameter Sensitivity Analysis

The influences of every TELB parameter on the soft-soil foundation embankment vary. Therefore, it is crucial to assess the sensitivity of each parameter to the embankment stability, as this provides a valuable theoretical reference for the TELB design.

The orthogonal test is a statistical method designed for analyzing multifactorial experiments. In such tests, the varying conditions of each factor under investigation are referred to as “levels”. For instance, in a formulation study, different concentrations (or proportions) of a component would constitute distinct levels.

To identify optimal production conditions, it is essential to examine multiple factors and their respective levels—a challenge known as multifactor optimization. The orthogonal test not only addresses this optimization problem but also enables researchers to evaluate the relative influence of each factor on experimental outcomes. This approach facilitates the identification of key factors, thereby streamlining the optimization process.

An orthogonal test was performed to study the influences of the TELB slope angle (A), lower edge width (B), height (C), density (D), internal friction angle (E), and cohesion (F) on the embankment stability. The orthogonal test table $L_{25}(5^6)$ consists of 6 factors and 5 levels. The 5-level factors are listed in Table 4. The results of every orthogonal factor combination case were obtained and shown in Table 5 through the numerical simulation. The numerical calculations were also performed employing FLAC software.

Table 4: Value and level for every factor

Level	Factors					
	TELB slope angle (A)/°	Lower edge width (B)/m	Height (C)/m	Density (D)/(kg·m^{-3})	Internal friction angle (E)/°	Cohesion (F)/kPa
1	85	3	2	1700	8	10
2	75	4	3	1800	12	12.5
3	65	5	4	1900	16	15
4	55	6	5	2000	20	17.5
5	45	7	6	2100	24	20

Table 5: The orthogonal test scheme

No.	Factors						
	TELB slope angle (A)/°	Lower edge width (B)/m	Height (C)/m	Density (D)/(kg·m^{-3})	Internal friction angle (E)/°	Cohesion (F)/kPa	F_s
1	85	3	2	1700	8	10	1.11
2	85	4	3	1800	12	12.5	1.13
3	85	5	4	1900	16	15	1.16
4	85	6	5	2000	20	17.5	1.18
5	85	7	6	2100	24	20	1.18
6	75	3	3	1900	20	20	1.14
7	75	4	4	2000	24	10	1.16
8	75	5	5	2100	8	12.5	1.18
9	75	6	6	1700	12	15	1.17
10	75	7	2	1800	16	17.5	1.14
11	65	3	4	2100	12	17.5	1.17
12	65	4	5	1700	16	20	1.16
13	65	5	6	1800	20	10	1.19
14	65	6	2	1900	24	12.5	1.14

(Continued)

Table 5 (continued)

No.	Factors						
	TELB slope angle (A)/°	Lower edge width (B)/m	Height (C)/m	Density (D)/(kg·m^{-3})	Internal friction angle (E)/°	Cohesion (F)/kPa	F_s
15	65	7	3	2000	8	15	1.17
16	55	3	5	1800	24	15	1.16
17	55	4	6	1900	8	17.5	1.19
18	55	5	2	2000	12	20	1.15
19	55	6	3	2100	16	10	1.18
20	55	7	4	1700	20	12.5	1.16
21	45	3	6	2000	16	12.5	1.19
22	45	4	2	2100	20	15	1.15
23	45	5	3	1700	24	17.5	1.13
24	45	6	4	1800	8	20	1.17
25	45	7	5	1900	12	10	1.19

Note: F_s is the stability coefficients.

The embankment stability coefficients are the largest for the four schemes ($A_3B_3C_5D_2E_4F_1$, $A_4B_2C_5D_3E_1F_4$, $A_5B_1C_5D_4E_3F_2$ and $A_5B_5C_4D_3E_2F_1$). Conversely, the scheme $A_1B_1C_1D_1E_1F_1$ yields the lowest embankment stability coefficient. Range analysis is used to evaluate how variations in key input parameters (e.g., TELB geometry, soil strength, loading conditions) influence the Factor of Safety (F_S). It quantifies the sensitivity of embankment stability to each parameter while holding others constant. The range analysis results of the orthogonal test are presented in Table 6.

Table 6: Range analysis results

	TELB slope angle (A)/°	Lower edge width (B)/m	Height (C)/m	Density (D)/(kg·m^{-3})	Internal friction angle (E)/°	Cohesion (F)/kPa
k_{1j}	1.152	1.154	1.138	1.146	1.164	1.166
k_{2j}	1.158	1.158	1.150	1.158	1.162	1.160
k_{3j}	1.166	1.162	1.164	1.164	1.166	1.162
k_{4j}	1.168	1.168	1.174	1.170	1.164	1.162
k_{5j}	1.166	1.168	1.184	1.172	1.154	1.160
R_j	0.016	0.014	0.046	0.026	0.012	0.006

Note: k_{1j} is the average of F_s for each factor at the same level; R_j is the range of the factor j.

As illustrated in Fig. 7, the embankment stability coefficients increase with the TELB slope angle decreasing while the lower edge width, height, and density increase. Among these parameters, height has the most pronounced effect on the stability coefficient, whereas cohesion has a minimal impact. This finding is consistent with the previously discussed results.

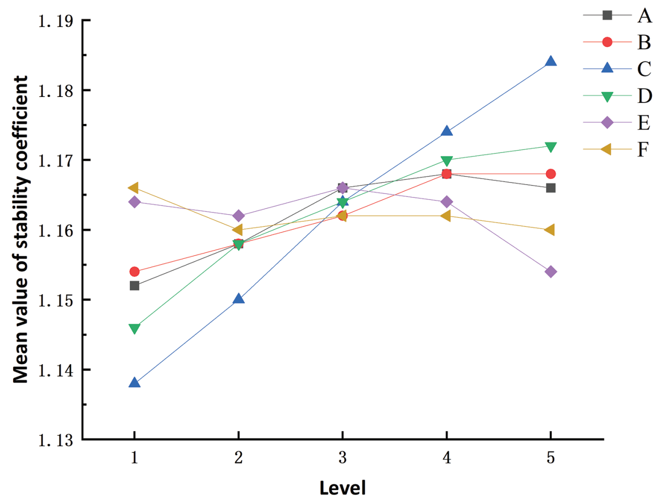

Figure 7: Average value of stability coefficients with different factors and levels. Slope angle (A), lower edge width (B), height (C), density (D), internal friction angle (E) and cohesion (F)

Fig. 8 depicts the range of stability coefficients for each factor. It is observed that $R_C > R_D > R_A > R_B > R_E > R_F$, which indicates that the height has the most significant influence on the embankment stability, followed by the density, slope angle, lower edge width, internal friction angle, and cohesion. Besides, the slope angle and lower edge width exert similar effects on the embankment stability. It is concluded that the embankment stability coefficients can be improved effectively by increasing the TELB density and height.

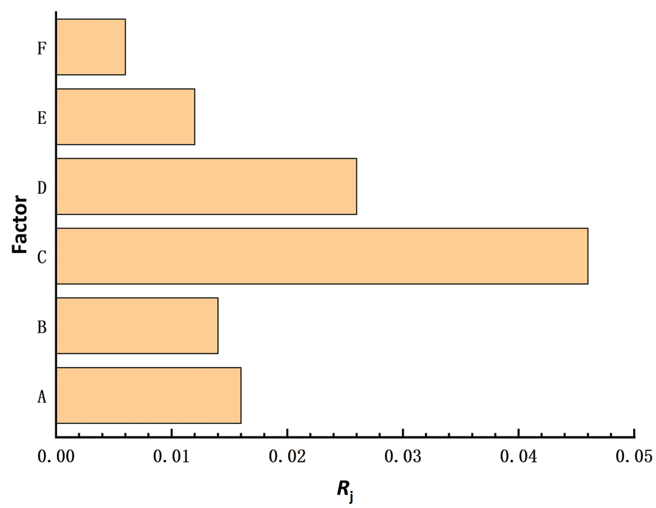

Figure 8: Range of the stability coefficient for every factor: slope angle (A), lower edge width (B), height(C), density (D), internal friction angle (E) and cohesion (F)

5 Conclusion

This paper introduces the trapezoidal embedded loading berm (TELB) as a method for reinforcing soft-soil foundation embankments. The feasibility of this approach was validated through both analytical and numerical analyses, and parameter sensitivity was evaluated using an orthogonal test. The following conclusions are drawn:

(1) An analytical model was developed to assess the stability of soft-soil foundation embankments reinforced by the TELB, demonstrating that the TELB effectively enhances stability.

(2) The stability coefficient of the soft-soil foundation embankment can be significantly influenced by the TELB width, height, and density. The stability coefficient can increase with these parameters increasing. However, the cohesion and internal friction angle has little influence on the stability coefficient.

(3) Among the TELB parameters, height exerts the most significant impact on embankment stability, followed by density, slope angle, lower edge width, internal friction angle, and cohesion. To improve the embankment stability coefficients, increasing the density and height is more effective.

This study focused on static loading conditions to establish a foundational understanding of the stability of embankments with rectangular embedded loading berms. However, as noted, seismic, dynamic traffic and cyclic hydraulic loads were not considered. These exclusions may limit the direct applicability of our findings to environments where dynamic or cyclic forces dominate, such as earthquake-prone regions, heavily trafficked infrastructure, or coastal systems subject to wave action. Future work should adopt pseudo-static or fully dynamic analysis.

Acknowledgement: Not applicable.

Funding Statement: This study was supported by the Natural Science Foundation of Anhui Province (Grant No. 2108085ME190), Xinjiang Key Laboratory of Geohazard Prevention (Grant No. XKLGP2023K02) and the Fundamental Research Funds for the Central Universities.

Author Contributions: Feng Xiong: Conceptualization (lead); Formal analysis (equal); Funding acquisition (lead); Methodology (equal); Writing—review & editing (equal). Yuexiang Wang: Formal analysis (equal); Methodology (supporting); Visualization (equal); Writing—review & editing (equal). Fan Yang: Formal analysis (equal); Methodology (equal); Visualization (equal); Writing—review & editing (equal). Lang Zhou: Data curation (equal); Investigation (equal); Validation (equal); Writing—review & editing (equal). Caifeng Hu: Project administration (equal); Validation (equal); Writing—review & editing (equal). Xuebing Wang: Project administration (equal); Validation (equal); Writing—review & editing (equal). Fan Li: Methodology (equal); Resources (equal); Validation (equal). All authors reviewed the results and approved the final version of the manuscript.

Availability of Data and Materials: The data that support the findings of this study are available from the corresponding author upon reasonable request.

Ethics Approval: Not applicable.

Conflicts of Interest: The authors declare no conflicts of interest to report regarding the present study.

References

1. Loktev A, Shishkina I, Savulidi M, Klekovkina N, Kuznetsov A. Justification of the parameters of a flexible grillage to strengthen the soft foundations of the subgrade of high-speed highways. Transp Res Procedia. 2022;63(2):825–35. doi:10.1016/j.trpro.2022.06.079.
2. Xing H, Xiong F, Wu J. Effects of pit excavation on an existing subway station and preventive measures. J Perform Constr Facil. 2016;30(6):04016063. doi:10.1061/(ASCE)CF.1943-5509.0000919.
3. Kaliakin VN, Al-Saadi ANS. Simulation of column supported embankments underlain by rigid and compressible soil layers. AIP Conf Proc. 2024;2864:030037. doi:10.1063/5.0186650.
4. Biradar V, Devappa VM, Jasutkar D, Sorate R, Kanase A, Desai A. Design of geosynthetic reinforced soil at slope failure and analysis of soil by various ground improvement techniques interface soil models. AIP Conf Proc. 2024;3139:070007. doi:10.1063/5.0224452.
5. Harabinova S, Panulinova E, Kormanikova E. Effect of soil material models on the prediction of earth embankment deformations. AIP Conf Proc. 2024;3094:170006. doi:10.1063/5.0212330.
6. Wanjari V, Patil P. Comparative probabilistic finite element analysis of cantilever retaining wall. AIP Conf Proc. 2024;3139:110004. doi:10.1063/5.0224644.
7. Huang R, Zhu J, Zhu XJ, Liu ZM. Analysis of ground settlement during shield tunnel construction in soft soil. Soil Mech Found Eng. 2023;60(2):134–40. doi:10.1007/s11204-023-09874-3.
8. Li X, Dong Z, Chen W, Wang J, Liu ZX, Li XB. Back analysis of a collapsed highway embankment—a numerical study on the rigid reinforcement and time-dependent grouting. Eng Fail Anal. 2022;131(8):105863. doi:10.1016/j.engfailanal.2021.105863.
9. Corkum AG, Martin CD. Analysis of a rock slide stabilized with a toe-berm: a case study in British Columbia Canada. International J Rock Mech Min Sci. 2004;41(7):1109–21. doi:10.1016/j.ijrmms.2004.04.008.
10. Zaytesv A, Petriaev A, Erniauskaite L. Track structure reconstruction practice for the subgrade on weak foundation soil. In: Proceedings of the Fifth International Conference on Road and Rail Infrastructure; 2018 May 17–19; Zadar, Croatia. doi:10.5592/CO/cetra.2018.972.
11. Liu JQ, Wang DL. Numerical analysis of back berm on road engineering with FEM. Adv Mater Res. 2013;748:1087–90. doi:10.4028/www.scientific.net/AMR.748.1087.
12. Zhu MS. Selection of reasonable cross-section of embankment in soft soil region. China Civ Eng J. 1964;2:48–60. (In Chinese). doi:10.15951/j.tmgcxb.1964.02.005.
13. Zhao NY, Liang B, Huang F, Liu Y. An analytical design method for loading berm of fill embankment. Rock Soil Mech. 2015;36(10):2914–20. (In Chinese). doi:10.16285/j.rsm.2015.10.022.
14. Chen JF, Song EX. Optimized design of loading berm for high fill slope of the airport in the mountainous area of southwest China. Eng Mech. 2012;29(6):85–91,97. (In Chinese). doi:10.6052/j.issn.1000-4750.2010.08.0610.
15. Viswanadham BVS, Das A, Mathur VK. Centrifuge model tests on rail embankments constructed with coal ash as a structural fill material. In: Proceedings of the GeoCongress 2012: State of the Art and Practice in Geotechnical Engineering; 2012 Mar 25–29; Oakland, CA, USA. doi:10.1061/9780784412121.388.
16. Zhang YD, Tan TS, Leung CF. Undrained end bearing capacity of an improved soil berm in an excavation. Soils Found. 2008;48(3):433–45. doi:10.3208/sandf.48.433.
17. Xiong F, Wang XB, Yang F, Yang JQ, Hu L, Li R. Analytical and numerical study on the stability of highway subgrade with embedded loading berm in soft soil area. Appl Sci. 2022;12(23):12440. doi:10.3390/app122312440.
18. Peng Z, Lan JW, Zhan LT, He HJ, Zheng XJ. Application of loading berm in landfill partial slip control. J Zhejiang Univ Eng Sci. 2018;52(4):710–8. doi:10.3785/j.issn.1008-973X.2018.04.014.